Super selective dual nature GO bridging PSF-GO-Pebax thin film nanocomposite membrane for IPA dehydration

Mohamad Syafiq Abdul Wahab , Sunarti Abd Rahman & Rozaimi Abu Samah

Published online: 23 Oct 2020.

Submit your article to this journal

Article views: 10

View related articles

View Crossmark data

Taylor & Francis
Taylor & Francis Group

Check for updates

Super selective dual nature GO bridging PSF-GO-Pebax thin film nanocomposite membrane for IPA dehydration

Mohamad Syafiq Abdul Wahab (ID), Sunarti Abd Rahman (ID), and Rozaimi Abu Samah (ID)

Department of Chemical Engineering, College of Engineering, Universiti Malaysia Pahang, Lebuhraya Tun Razak, Gambang, Kuantan, Pahang, Malaysia

ABSTRACT

In this work, Graphene Oxide (GO) is embedded in both selective hydrophilic layer and porous hydrophobic substrate creating a mutual bridge between the two surfaces. Pristine 1–3 µm microporous PSF prepared via dry/wet phase inversion techniques with contact angle of 74.12° has been further study with GO embedded Pebax dense selective layer. This dual nature thin film nano composite TFNC membranes managed to reduce the water contact angle down to 37.18°. As for the IPA dehydration study, the total flux up to 1.19 kgm^{-2}h^{-1} and 0 wt% IPA detected in permeate was achieved with 20 wt% water feed at 30°C.

1. Introduction

Pervaporation (PV) is among the greenest system in chemical purification industries. The name itself defines the process; permeation and vaporization, at which the permeating species is forced to vaporize on the other side of the membrane. A closed vacuum system subsequently lowers the boiling point of the binary feed, vaporizing the permeate species easily even at room temperature. This low-cost separation process offers an alternative way to the current azeotropic binary separation with its low energy requirement and the flexibility of the membrane synthesis to tackle every permeating components. At certain condition, organic binary mixture will reach a very specific point where they no longer can be separated by simple distillation method. Isopropyl Alcohol (IPA) and water formed an azeotropic mixture at 87.4 wt% and the mixture boiling point (b.p) is lowered down to 80.4°C compared to individual b.p of IPA (82.5°C) and water (100°C).[1] As the IPA purity is to be concerned for most of its application, membrane pervaporation seems the most promising compared to the others without any entrainer usage such the one in azeotropic or extractive distillation practice, which later another separation method should be carried out to remove the entrainer.

Over the decades, hydrophilic-based polymers such as PVA, and amine functionalized polymers have been utilized for this purpose, yet the long addressed 'trade off 'is still there, where the permeable the polymers are,, the

less selective it could be and vice versa. As most of the organic mixtures are polar molecule that easily permeate through hydrophilic membranes surface creating a temporary hydrogen bonding during the separation process, making it vulnerable when in contact with high water content. Having so, both species are allowed to permeate through, reducing the selectivity of the desired components.

This work study, a progressive synthesis of PSF-GO-Pebax TFNC which begins with the core part of the active dense layer of Pebax by varying the copolymer concentration, followed by the addition of GO as the hydrophilic enhancer to the active layer and later the modification of hydrophobic PSF support with GO embedded structure to further increase the permeate flux. PSF was selected as the support to the TFNC due to its hydrophobicity compared to Pebax, porous, and amorphous nature providing a less swell surface when in contact with water. Past study showed that modified PSF is among the best material in PV with notable water selectivity and its resistivity to organic solvents. Many have tried to introduce hydrophilic moieties to PSF via crosslinking, nanomaterial or surface modification such as addition of ammonium,[2] nano iron,[3] zeolite[4] and sulfonated,[5] by any means, disruption of polymer packing is the current focused of PV membrane development. Huang et al., 1999 mentioned, dual nature composite membrane of hydrophobic and hydrophilic materials resulting in an instability of membrane structure from the surface tension difference,[6] so it is crucial

---

CONTACT Sunarti Abd Rahman ✉ syafiqmohamad82@gmail.com 🖃 Faculty of Chemical & Process Engineering Technology, College of Engineering Technology, Universiti Malaysia Pahang, Kuantan, Pahang 26300, Malaysia

Table 1. Pebax related works on organic binary separation.

Materials	Binary Solution	Flux, kg/m^2.h	References
Pebax/POSS	Ethanol/water	0.1835	[10]
PEBA/ceramic	N butanol/water	4.196	[11]
PEBA/MOF	Ethanol/water	4.446	[12]
ZSM-5/PEBA/PES	ethyl acetate/water	1.895	[13]
chitosan/poly(ether-block-amide)	NMP/Water	0.019	[14]
Pebax-GO-PSF	IPA/Water	1.19	This work

for researchers to find the best nanomaterials that not only water selective but can link the two properties well.

Pebax on the other hand has been widely used in gas separation application. This dense polar ether containing block copolymers having the best of the both worlds, hard segment of polyamide (PA) provide a robust structure and high thermal resistant, while the PEO has an excellent CO_2 solubility.[7–9] These two phases crystalline and amorphous microscopic scale copolymer imparts both thermoplastic and elastomers characteristic. In liquid separation, Pebax started to get researchers' attention showing a significant progress in alcohol dehydration. Table 1 summarizes the current progress of Pebax in organic binary separation.

GO is introduced in this study, bridging the two nature of hydrophilic Pebax selective layer and the porous hydrophobic PSF. The addition of this 2D nanomaterials is believed could improve the flux rate and water selectivity. These nanomaterials proven through several studies on the effectiveness of water uptakes, with the large surface area combining with multiple possible H-bonding functional group, making GO the best candidates to be considered in TFNC development. From morphological view, presence of GO obstruct crystallization by reducing nucleation site of the polymer matrix creating a less compact matrix, reducing the degree of crystallinity, yet providing good water transport for permeation through the selective nano scale channel of the interlayer spacing.

2. Methodology

2.1. Materials

Polysulfone (PSF) was supplied by Gardner Global, Polyether block amide (Pebax) was supplied by Arkema France under trade name Pebax MH 1657 and graphene oxide, GO (763713–1 G) was supplied by Sigma Aldrich. Solvents used in this study, isopropyl alcohol (IPA) with 99.98% purity was supplied by HmbG Chemicals, 99.9%

ethanol, and Dimethylformamide (DMF) was supplied by Sigma Aldrich.

2.2. Pristine PSF film

15 wt% of PSF was dissolved in 85 wt% of DMF and mechanically stirred with an overhead stirrer for 6 hours at 80°C until a clear homogenous dope solution is attained. After being degassed at room temperature for 24 hours, the dope was casted on a glass plate using a 0.03 mm knife blade and it was immediately transferred to a water bath for 2 h. The cast film was then dried overnight at room temperature.

2.3. Pebax-PSF-GO TFNC

Pebax (1–5 wt %) was dissolved in ethanol–water mixture with ratio of 70:30 and stirred at 60°C for 4 hours. The homogenous solution was then coated on pristine PSF film by dip coating techniques. For the final curing, the TFC was oven overnight at 60°C before being tested with IPA dehydration study as illustrated in Figure 1.

For the effect of GO loading study, 0.005 g/ml GO in water was prepared as a stock solution, and it was loaded to 3 wt% of Pebax in range of 0.05 wt% to 0.5 wt% before being coated on the PSF pristine. To study the effect of GO on PSF substrate, 0.005 g/ml GO in DMF was prepared and it was dispersed to PSF dope in range of 0.2 wt % to 1 wt%. The GO-PSF dope was then ultrasonicated at 60°C for 24 hours before being casted.

2.4. Characterization

The cross-sectional area of the samples was examined by Carl Zeiss scanning electron microscope (SEM). To avoid shear effect and cutting blockage, the samples were frozen and fractured in liquid nitrogen and flushed with a platinum coating by JEOL Auto Fine Coater JFC-
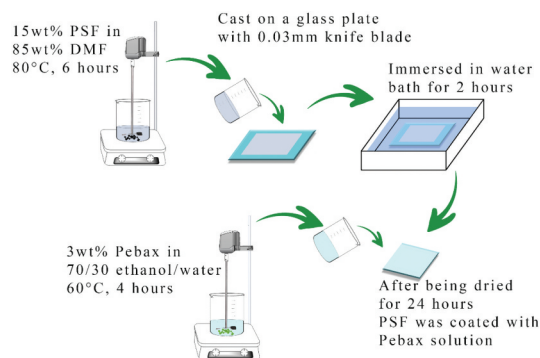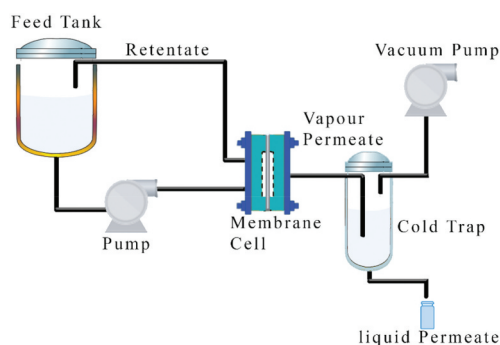

Figure 1. PSF-Pebax TFC synthesis.

Figure 2. Pervaporation system.

1600. For functional group detection, all films were examined by Fourier transform infrared spectroscopy (FTIR) Nicolet™ iS™ 5 FTIR Spectrometer. The characteristic beam of different wavelength was then analyzed in Omnic 9.5.9. The thermal stability and degradation of TFNC membrane were investigated by high resolution thermogravimetric analysis (TA instrument TGA Q500), performed between 25 and 800°C, heating rate of 5 K/min under nitrogen flux (60 ml/min). X-ray diffraction analysis (XRD) is employed for polymeric crystallinity and phases study via Philips X'Pert-MPD X-ray Diffraction System. The method used is as follows; $\lambda = 1$ Å; angle of incidence = 2θ; scanning range = $10°$–$80°$; scanning speed = $0.1°$/s. Hydrophilicity of the samples was measured based on water contact angle to the film surface, angle less than $90°$ and leaning toward $0°$ indicates the film is increasing its affinity for water and vice versa.

2.5. IPA dehydration by membrane pervaporation

Pervaporation system for this study is illustrated as in Figure 2, 200 ml IPA-Water binary mixture was fed to a 1 l feed tank and it was pump at 1 l/min rate to a 0.00385 m^2 prefixed membrane. The permeate was collected in an evacuated cold trap at a 55 mmHg and weighed on a Shimadzu AY220 weighing balance. Permeate composition was determined by Atago Pocket Refractometer, PAL-37s for permeate with 0 to 0.6 wt% of IPA, and FTIR absorbance for IPA less than 0.9 wt%. The total permeation flux (j) and selectivity (α) was calculated by the following equations;

$$j = \frac{wA}{t} \tag{1}$$

Where j is total permeation flux in kg/m^{2}h, w is the permeate mass in kg, A is the membrane surface area in m^2 and t is the permeation time in h. Separation factor (α) is defined as:

$$\alpha = \frac{y_P/y_f}{x_P/x_f} \tag{2}$$

Where xf and yf are weight fractions of water and organic compound in feed and xp and yp are weight fractions of water and organic compound in permeate streams.

3. Results and discussion

3.1. Characterization

SEM micrograph of the produced membrane are presented in Figure 3. Pristine PSF support showed a symmetric porous structure ranging from 1 to 3 μm. The effect of solvent-nonsolvent demixing creates a uniform spongy microporous channel from bottom to the surface. The formation of finger like microvoid was strongly believed due to faster solvent demixing. Solvent-non solvent demixing rate is more related to polymer viscosity,[15,16] indicates an appropriate amount of polymer loading – 15 wt% of PSF. It can be concluded that 15 wt% is high enough to ensure rapid demixing urge for voids formation. These voids helped in increasing permeate flux by reducing the diffusion path length and creating a lower tortuosity. As we all know, permeation flux in a porous media is inversely proportional to membrane thickness and its tortuosity.[17] Having a finger-like microvoids avoids the formation of unnecessary irregular porosity, twisted and unconnected pore which disturb the permeate diffusion.

Asymmetric dense-porous PSF-Pebax TFC in Figure 3b clearly indicates the 930 nm selective thin boundary of Pebax coating. For the SEM provided, the PSF was coated with 3 wt% Pebax, which is the best loading among all. Some of the Pebax might have penetrated deeper into the porous structure leaving a dense flake clutter in the PSF porous region. Adding of GO to the selective layer, introduced a rougher surface, creating a nodular aggregation that can be clearly seen in Figure 3c,d. this is a good sign; the rougher surface increases the absorption site. We can see an obvious change in porous network formation of GO embedded PSF in Figure 3d. GO interrupt the porous structure, eliminate finger-like microvoid but introducing a compact shorter path, making it thinner from 103 μm (pristine PSF) to 46 μm in thickness.

FTIR spectra of the TFNC is given in Figure 4 together with pristine PSF film as a reference for the produced film. Three characteristic functional group should be observed in PSF contains film, aromatic, sulfonyl and alkyl. Strong symmetric stretching of -SO$_2$ sulfonyl from the PSF substrate was detected at

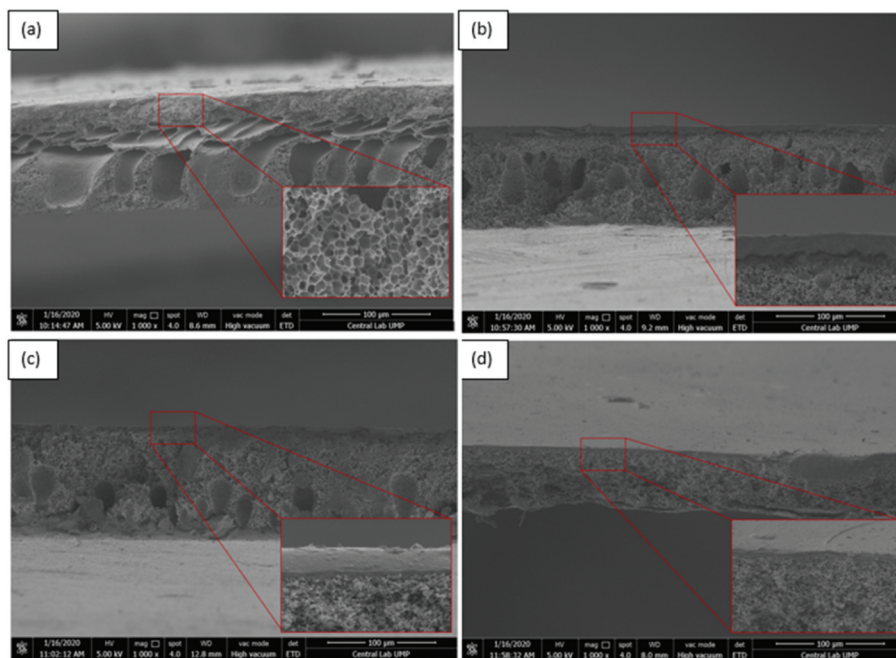**Figure 3.** SEM micrograph of (a) pristine PSF film, (b) Pebax-PSF TFC, (c) GO embedded Pebax-PSF TFNC, (d) PSF-GO-Pebax TFNC.
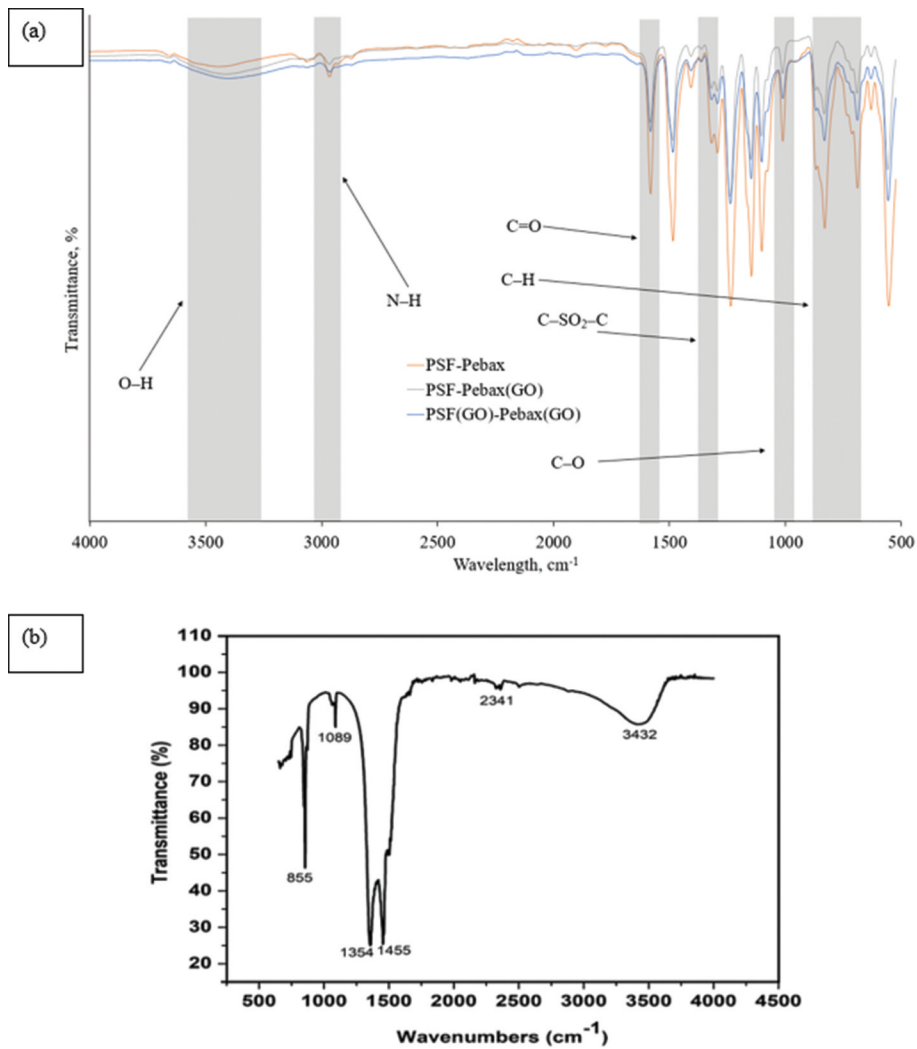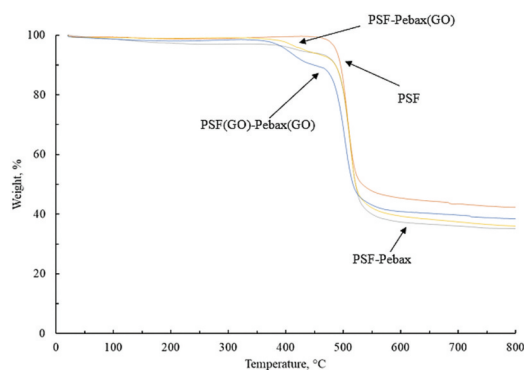

Figure 4. FTIR spectra of (a) various film produced in this study (b) PSF film[18].

Figure 5. TGA analysis for PSF, PSF-Pebax, PSF-Pebax(GO) and PSF(GO)-Pebax(GO).

1350 cm^{-1}. The characteristic bands at 690 and 855 cm^{-1} are aromatic CH bending. Characteristic peak of the PSF region produced film is identical to the one described by Naz et al.[18] A broad -OH stretching at around 3400–3500 cm^{-1} is attributed to the carboxyl of GO and the one in Pebax. The intensity increase as the amount of GO loaded to the PSF-Pebax(GO) to PSF(GO)-Pebax(GO) increase, reflecting the peak depth different at 3475 cm^{-1}. It proved that more -OH moieties are present in the samples. The Fermi resonant N-H stretch vibration of the amide (H bonded NH) can be spot at 3070 cm^{-1}, while C = O can be spotted at around 1600 cm^{-1}. It was said that any spectrum falls in between 2800 and 3200 cm^{-1} involved in bonding congestion of cis amide between water and ammonia.[19]

The thermogravimetric analysis curves for all the films was given in Figure 5. All modified samples start losing weight at around 364°C with two steps thermal decomposition which later occurs at the same point as Pristine PSF did, at 464°C. The first drop is attributed to the decomposition of unstable oxygen functionality of both GO and dense Pebax surface. The major weight loss at 464°C for all the samples was due to the decomposition of PSF
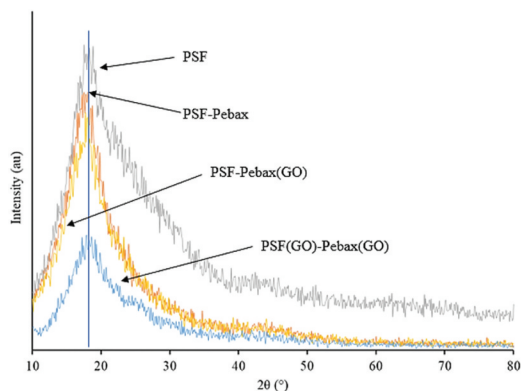
backbones. As more oxygen atom is added to the structure, it weakens the polymer backbone and lead to oxidative degradation.[20] It proved that adding more hydrophilic moieties fasten the degradation rate with respect to temperature. Even though there is a slight decrease in decomposition temperature for the modified membranes compared to pristine PSF, the modified membranes still can be used in IPA dehydration because the operating temperature can be as low as room temperature.

Figure 6 shows the XRD patterns of PSF, PSF-Pebax, PSF-Pebax(GO) and PSF(GO)-Pebax(GO). The significant peak at 2θ = 18° belongs to the PSF.[21–23] All of the modified films showing similar peak, proving that adding Pebax and GO to the Pristine PSF film does not affect the amorphous nature of the films. However, the intensity of the PSF peak decreases as amount of the modification by adding Pebax and GO increases, this might be due to the intercalation of GO flakes in PSF matrix, reducing the membrane-free volume. Many have agreed that adding filler or particles reducing the polymer chain and disrupt the polymer packing thus decreasing the crystallization of the polymer backbone.

3.2. Water contact angle

Contact angle of the film is given in Figure 7. Surface hydrophilicity of the membranes was reduced down to 37.18 ° via Pebax coating. Pebax was known for its hydrophilic surface that make them favorable for water selective application. A notable rise to some degrees was observed when GO was loaded into the film configuration. The rise is a response to the changes of surface energy and intra molecular hydrogen bonding within the polymer matrix.[24]

3.3. Effect of Pebax selective layer concentration

Figure 8 shows the effect of Pebax selective layer contents for PSF-Pebax TFC on flux rate and water

Figure 6. XRD patterns of various film studied.
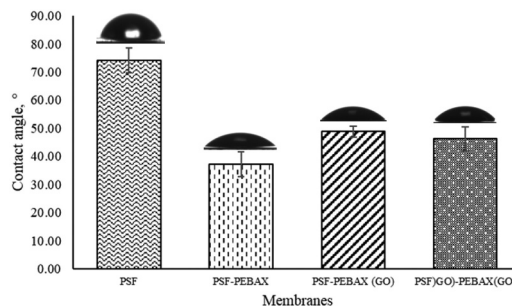
**Figure 7.** Contact angle of various film configuration.
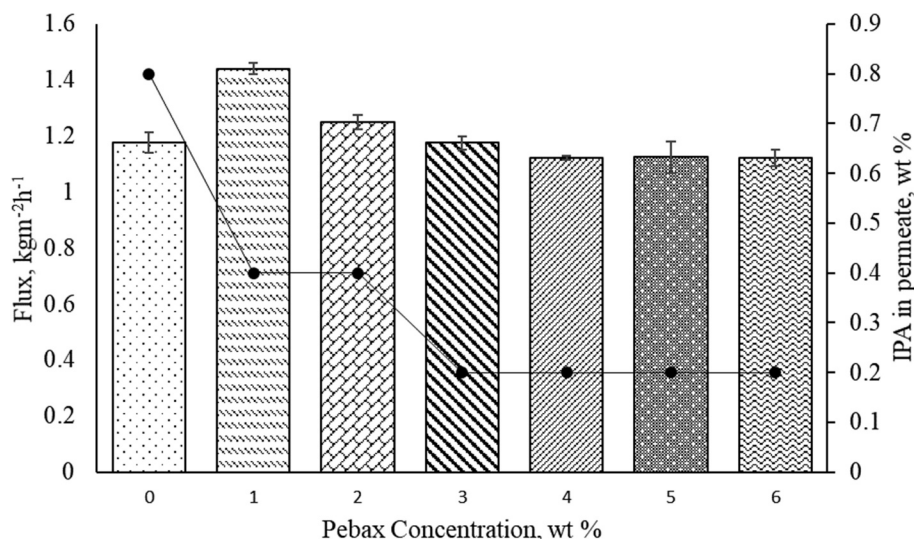
Figure 8. Effect of Pebax selective layer contents in PSF-Pebax TFC on Flux and water selectivity at 30℃, 20 wt % water contents in feed.

selectivity. The flux decreases with the increasing amount of Pebax loading on the selective layer. As the loading increases, the amount of crystalline hard segment PA introduced to the porous PSF substrate increases significantly thus blocking the water diffusion channel. Increase in selective layer concentration also leads to a thicker dense layer formation, not just that, it increases mass transfer-resistant for the permeate. A significant drop in IPA contents in permeate can be observed as Pebax concentration increase throughout the film preparation from 0.4 to 0.2 and later remain stagnant from 3 wt% to 6 wt%. The highly mobile ether linkage of PE segment provides more sorption site for water molecule and it reaches its limit with 3 wt% polymer loading. Polar oxygenated ether terminal selectively forms hydrogen bonding with polar water molecule over the less polar IPA. So, there is a limit for the Pebax selective layer to only allow water to absorb through, corresponding to possible -H linkage.

3.4. Effect of GO dispersed in Pebax selective layer

For the effect of GO dispersion on Pebax selective layer study, GO was dispersed into 3 wt% Pebax with various loading as in Figure 9. The study aims to reduce IPA contents in permeate thus boosting the water selectivity of the produced film. When GO is added to the selective layer, more hydrophilic moieties are introduced to the surface. By doing so, multiple polar terminals within GO flakes can form hydrogen bonding with water. This PSF-Pebax(GO) film reaches its limit with 0.5 wt% of GO loading with flux of 1.039 $kgm^{-2}h^{-1}$. For this experiment, no alcohol traces were found in all of the samples.

To understand more on this surface absorption behavior, take a look at Figure 10. GO bearing large
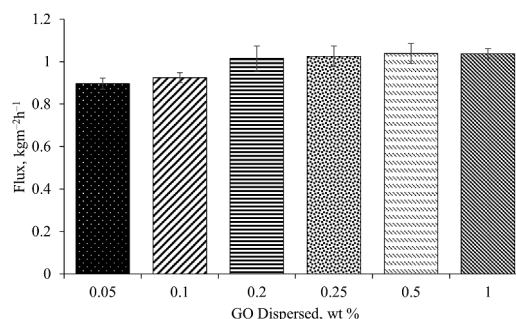
Figure 9. Effect of GO dispersion on Pebax selective layer toward water flux.
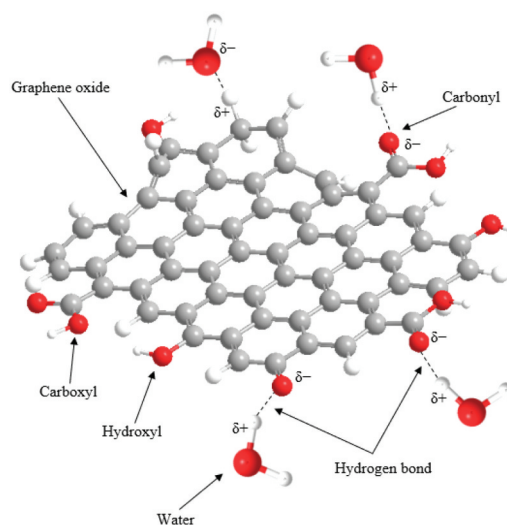
Figure 10. 3D representation of GO-water possible attraction during IPA dehydration via GO embedded Pebax TFNC.

H bonding possibilities, with every terminal holds at least one electronegative O atom which easily attracts the partially positive charge of H atom of the water molecule. Not just that, water too forms weak H-bonding with another charged terminal, such as the carboxyl (–COOH). This special dipole-dipole attraction is a weaker intermolecular bonding compared to ionic and covalent, taking advantage of the polar rich GO structure, it helps in creating selective absorption site for the separation process.

3.5. Effect of Pebax-GO selective layer thickness

A drop in flux (Figure 11) can be seen as selective layer is increased throughout the study. This phenomenon can be explained by flux (j_w) and membrane parameter relation found in several studies, where;

$$j_w \propto \frac{r^\alpha \varepsilon}{\tau \delta} \tag{3}$$

Flux is directly proportional to pore size (r^α), porosity, or void volume fraction (ε) but inversely proportional to pore tortuosity (τ) and thickness (δ).[25,26] Increasing in number of coating layer alters both the physical parameter of the film-thickness and tortuosity. Having a thicker dense selective layer increases the mass transfer-resistant, thus slowing the flux rate, and it does not affect the water selectivity. Meaning selectivity is an independent variable of selective layer thickness. Based on this study, a clear judgment in PV can be made that permeate concentration of a dense membrane is independent of vapor-liquid equilibrium (VLE) which often related to distillation, but solely tied to solubility and diffusivity of permeate species and the selective materials.

3.6. Effect of GO dispersed in PSF support of Pebax-GO TFNC

The flux data for this TFNC configuration are presented in Figure 12. This configuration was proposed
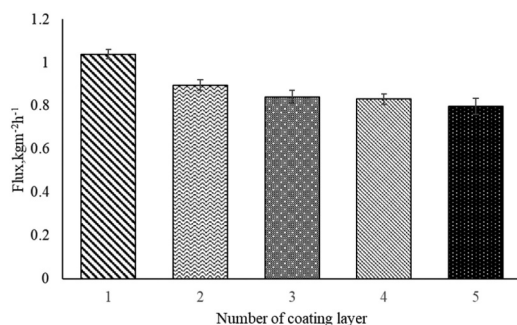
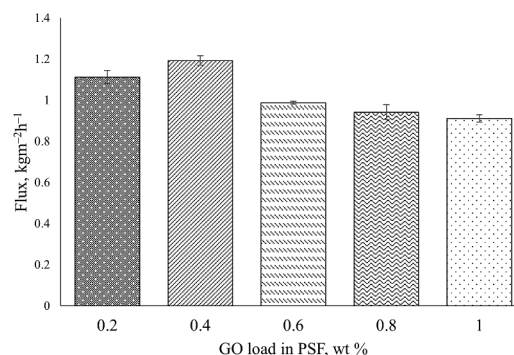**Figure 11.** Effect of coating layer to flux rate.

Figure 12. Effect of GO loading in the PSF substrate.

as an answer to the interlayer effect in composite membranes. Lilleparg et al., 2019 said in their work that, for a thin film composite membrane, there is more than the layer thickness that affects the flux, but the interaction of the layers also contributes to the film efficiency.[17] The interlayer effect or incompatibility was overcome through this mutual bridging, water molecule was selectively absorbed at the dense selective surface and it was diffused through to the porous support via GO bridging which embedded in both layers. The effective separation of this configuration is not governed only by the free volume within polymer macromolecular chain but the synergetic effect of GO between the surfaces. However, a drop in flux can be seen as GO load increase to 0.6 wt% and beyond, this can be related to excessive loading and pore blockage. Similar trends on GO works also can be seen elsewhere when the loading goes beyond 0.5 g/L.[27]

The dual nature surface of Pebax and PSF creates adhesive forces in between, and causes the liquid to cling in the middle, instead of flowing through in a droplet form, the permeating liquid spread over the interlayer surface and causing what often called 'wetting'. Rezaei et al., 2018 ascribed pore wetting as deposition of any organic or non-organic compounds on a membrane surface that affects permeate quality and flux flow.[28] Even though there is research saying that, membranes with high adhesive forces might be good for selective transportation, but, in the case of composite film this cannot be applied.[29] The delayed in flux transmission between the two surfaces due to surface tension difference creating water boundary which is less desired for it is hardly to channel through. Role of GO is presented graphically in Figure 13. Adding GO to PSF matrix ignored the cohesive forces among the permeating water through its mutual bridging. Water can be easily passing through the PSF surface via GO active groups, so surface wetting can

(a)

(b)
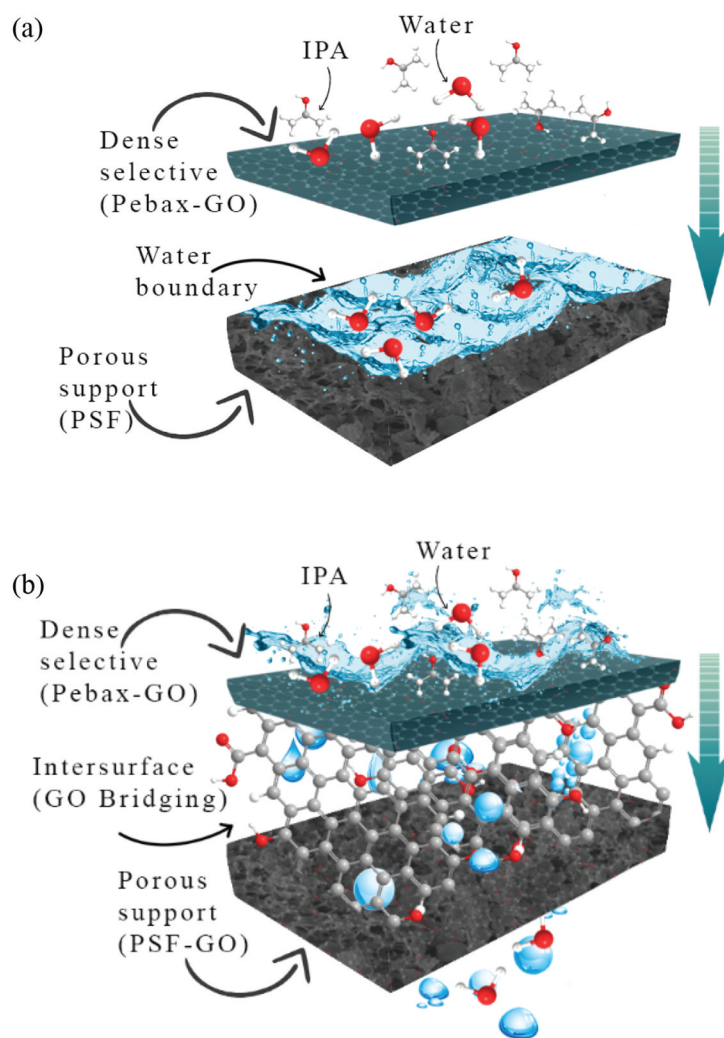
Figure 13. (a) Water boundary formation on TFNC with PSF support (b) GO mutual bridging in PSF-GO-Pebax TFNC.

be reduced. This theory actually makes sense, even though permeating water is in 'bead' form due to different surface nature, the transportation still occurs via GO polar terminals.

mutual bridging PSF-GO-Pebax on the other hand managed to score a higher flux at 1.19 kgm^{-2}h^{-1} and 0 wt% IPA traces with only 0.4 wt% of GO loading to the PSF matrix.

4. Conclusion

A mutual bridging PSF-GO-Pebax TFNC was successfully synthesized to completely eliminate IPA traces in IPA dehydration permeate. There is a significant improvement for every study made, for the effect of Pebax concentration in PSF-Pebax composite, 1.17 kgm^{-2}h^{-1} and 0.2 wt% IPA in permeate was recorded with 3 wt% Pebax concentration. As the study grows, GO was added to reduce the IPA traces, and flux of 1.04 kgm^{-2}h^{-1} and IPA was completely separated from the permeate. It was found that having a thicker selective layer gave a negative effect for the flux rate and maintaining the 0 wt% alcohol traces in permeate. The novel

Notes on contributors

Dr. *Mohamad Syafiq Abdul Wahab* is a researcher in the area of polymeric membrane development and was based in

Universiti Malaysia Pahang, Malaysia. His work mostly related to pervaporation and gas separation.

A.P Ts. Dr. Sunarti Abd Rahman is an associate professor that has been working in various polymeric membrane research for the past 15 years. She is an expert in polymeric membrane synthesis, membrane contactor, gas and liquid separation, and a few areas of absorption and adsorption. Aside from the research work, she is currently a lecturer in the separation process, fluid mechanics, and few other related chemical engineering subjects offered in Universiti Malaysia Pahang, Malaysia.

Dr. *Rozaimi Abu Samah* is a senior lecturer in Universiti Malaysia Pahang, Malaysia. His interest is in the area of enzymes and microbiology. He is currently exploring the area of the separation process for bioproducts and biomass waste utilization.

ORCID

Mohamad Syafiq Abdul Wahab 🔟 http://orcid.org/0000-0001-5107-8631
Sunarti Abd Rahman 🔟 http://orcid.org/0000-0003-0986-5548
Rozaimi Abu Samah 🔟 http://orcid.org/0000-0003-3124-0595

References

[1] Itoh, N.; Ishida, J.; Kikuchi, Y.; Sato, T.; Hasegawa, Y. Continuous Dehydration of IPA–water Mixture by Vapor Permeation Using Y Type Zeolite Membrane in a Recycling System. *Sep. Purif. Technol.* 2015, *147*, 346–352. DOI: 10.1016/j.seppur.2014.12.021.

[2] Liou, R.-M.; Chen, S.-H.; Lai, C.-L.; Hung, M.-Y.; Huang, C.-H. Effect of Ammonium Groups of Sulfonated Polysulfone Membrane on Its Pervaporation Performance. *Desalination.* 2011, *278*, 91–97. DOI: 10.1016/j.desal.2011.05.006.

[3] Chen, S.-H.; Liou, R.-M.; Lai, C.-L.; Hung, M.-Y.; Tsai, M.-H.; Huang, S.-L. Embedded Nano-iron Polysulfone Membrane for Dehydration of the Ethanol/water Mixtures by Pervaporation. *Desalination.* 2008, *234*, 221–231. DOI: 10.1016/j.desal.2007.09.089.

[4] Fu, Y.-J.; Hu, -C.-C.; Lee, K.-R.; Lai, J.-Y. Separation of Ethanol/water Mixtures by Pervaporation through Zeolite-filled Polysulfone Membrane Containing 3-aminopropyltrimethoxysilane. *Desalination.* 2006, *193*, 119–128. DOI: 10.1016/j.desal.2005.07.049.

[5] Chen, S.-H.; Yu, K.-C.; Lin, -S.-S.; Chang, D.-J.; Liou, R. M. Pervaporation Separation of Water/ethanol Mixture by Sulfonated Polysulfone Membrane. *J. Membrane Sci.* 2001, *183*, 29–36. DOI: 10.1016/S0376-7388(00)00544-5.

[6] Huang, R. Y. M.; Pal, R.; Moon, G. Y. Crosslinked Chitosan Composite Membrane for the Pervaporation Dehydration of Alcohol Mixtures and Enhancement of Structural Stability of Chitosan/polysulfone Composite Membranes. *J. Membrane Sci.* 1999, *160*, 17–30. DOI: 10.1016/S0376-7388(99)00074-5.

[7] Meshkat, S.; Kaliaguine, S.; Rodrigue, D. Comparison between ZIF-67 and ZIF-8 in Pebax® MH-1657 Mixed Matrix Membranes for CO2 Separation. *Sep. Purif. Technol.* 2020, *235*, 116150. DOI: 10.1016/j.seppur.2019.116150.

[8] Liu, Y.-C.; Chen, C.-Y.; Lin, G.-S.; Chen, C.-H.; Wu, K. C. W.; Lin, C.-H.; Tung, K.-L. Characterization and Molecular Simulation of Pebax-1657-based Mixed Matrix Membranes Incorporating MoS2 Nanosheets for Carbon Dioxide Capture Enhancement. *J. Membr. Sci.* 2019, *582*, 358–366. DOI: 10.1016/j.memsci.2019.04.025.

[9] Farashi, Z.; Azizi, S.; Rezaei-Dasht Arzhandi, M.; Noroozi, Z.; Azizi, N. Improving CO2/CH4 Separation Efficiency of Pebax-1657 Membrane by Adding Al_2O_3 Nanoparticles in Its Matrix. *J. Nat. Gas. Sci. Eng.* 2019, *72*, 103019. DOI: 10.1016/j.jngse.2019.103019.

[10] Le, N. L.; Wang, Y.; Chung, T.-S. Pebax/POSS Mixed Matrix Membranes for Ethanol Recovery from Aqueous Solutions via Pervaporation. *J. Membrane Sci.* 2011, *379*, 174–183. DOI: 10.1016/j.memsci.2011.05.060.

[11] Li, Y.; Shen, J.; Guan, K.; Liu, G.; Zhou, H.; Jin, W. PEBA/ceramic Hollow Fiber Composite Membrane for High-efficiency Recovery of Bio-butanol via Pervaporation. *J. Membrane Sci.* 2016, *510*, 338–347. DOI: 10.1016/j.memsci.2016.03.013.

[12] Liu, Q.; Li, Y.; Li, Q.; Liu, G.; Liu, G.; Jin, W. Mixed-matrix Hollow Fiber Composite Membranes Comprising of PEBA and MOF for Pervaporation Separation of Ethanol/water Mixtures. *Sep. Purif. Technol.* 2019, *214*, 2–10. DOI: 10.1016/j.seppur.2018.01.050.

[13] Vatani, M.; Raisi, A.; Pazuki, G. Mixed Matrix Membrane of ZSM-5/poly (Ether-block-amide)/polyethersulfone for Pervaporation Separation of Ethyl Acetate from Aqueous Solution. *Microporous Mesoporous Mater.* 2018, *263*, 257–267. DOI: 10.1016/j.micromeso.2017.12.030.

[14] Prasad, N. S.; Moulik, S.; Bohra, S.; Rani, K. Y.; Sridhar, S. Solvent Resistant Chitosan/poly(ether-block-amide) Composite Membranes for Pervaporation of N-methyl-2-pyrrolidone/water Mixtures. *Carbohydr. Polym.* 2016, *136*, 1170–1181. DOI: 10.1016/j.carbpol.2015.10.037.

[15] Idris, A.; Man, Z.; Maulud, A.; Khan, M. Effects of Phase Separation Behavior on Morphology and Performance of Polycarbonate Membranes. *Membranes.* 2017, *7*(2), 21. DOI: 10.3390/membranes7020021.

[16] Ismail, A.; Khulbe, K.; Matsuura, T. RO Membrane Preparation. *Reverse Osmosis.* 2019, 25–56. DOI: 10.1016/b978-0-12-811468-1.00002-5.

[17] Lillepärg, J.; Breitenkamp, S.; Shishatskiy, S.; Pohlmann, J.; Wind, J.; Scholles, C.; Brinkmann, T. Characteristics of Gas Permeation Behaviour in Multilayer Thin Film Composite Membranes for CO_2 Separation. *Membranes.* 2019, *9*. DOI: 10.3390/membranes9020022.

[18] Naz, M.; Ahmad, S.; Shukrullah, S.; Altaf, N.; Ghaffar, A. Effect of Microwave Plasma Treatment on Membrane Structure of Polysulfone Fabricated Using Phase Inversion Method. *Mater Today-Proc.* 2020. DOI: 10.1016/j.matpr.2020.04.522.

[19] Fedorov, A.; Cable, J.; Carney, J.; Zwier, T. Infrared Spectroscopy of H-Bonded Bridges Stretched across thecis-Amide Group: II. Ammonia and Mixed Ammonia/Water Bridges. *J. Phys. Chem. A.* 2001, *105*, 8162–8175. DOI: 10.1021/jp011178q.

[20] Yang, B.; Mao, J.; Zhao, J.; Shao, Y.; Zhang, Y.; Zhang, Z.; Lu, Q. Improving the Thermal Stability of Hydrophobic Associative Polymer Aqueous Solution Using a "Triple-protection" Strategy. *Polymers.* 2019, *11*, 949. DOI: 10.3390/polym11060949.

[21] Anastasiou, S.; Bhoria, N.; Pokhrel, J.; Kumar Reddy, K. S.; Srinivasakannan, C.; Wang, K.; Karanikolos, G. N. Metal-organic Framework/graphene Oxide Composite Fillers in Mixed-matrix Membranes for CO_2 Separation. *Mater. Chem. Phys.* 2018, *212*, 513–522. DOI: 10.1016/j.matchemphys.2018.03.064.

[22] Alosaimi, A. M.; Hussein, M. A.; Abdelaal, M. Y.; Elfaky, M. A.; Sobahi, T. R.; Abdel-Daiem, A. M. Polysulfone-based Modified Organoclay Nanocomposites as a Promising Breast Anticancer Agent. *Cogent Chem.* 2017, *3*. DOI: 10.1080/23312009.2017.1417672.

[23] Sun, J.-T.; Wang, -C.-C.; Lee, H.-T.; Wu, C.-L.; Gu, J.-H.; Suen, M.-C. Preparation and Characterization of Polysulfone/Nanosilver-Doped Activated Carbon Nanocomposite. *Polym. Sci. Ser. A.* 2018, *60*, 90–101. DOI: 10.1134/S0965545X18010054.

[24] Liao, Y.-L.; Hu, -C.-C.; Lai, J.-Y.; Liu, Y.-L. Crosslinked Polybenzoxazine Based Membrane Exhibiting In-situ Self-promoted Separation Performance for Pervaporation Dehydration on Isopropanol Aqueous Solutions. *J. Membrane Sci.* 2017, *531*, 10–15. DOI: 10.1016/j.memsci.2017.02.039.

[25] Woods, J.; Pellegrino, J.; Burch, J. Generalized Guidance for considering Pore-size Distribution in Membrane Distillation. *J. Membrane Sci.* 2011, *368*, 124–133. DOI: 10.1016/j.memsci.2010.11.041.

[26] Phattaranawik, J.; Jiraratananon, R.; Fane, A. G. Effect of Pore Size Distribution and Air Flux on Mass Transport in Direct Contact Membrane Distillation. *J. Membrane Sci.* 2003, *215*, 75–85. DOI: 10.1016/S0376-7388(02)00603-8.

[27] Choi, H.-G.; Shah, A. A.; Nam, S.-E.; Park, Y.-I.; Park, H. Thin-film Composite Membranes Comprising Ultrathin Hydrophilic Polydopamine Interlayer with Graphene Oxide for Forward Osmosis. *Desalination.* 2019, *449*, 41–49. DOI: 10.1016/j.desal.2018.10.012.

[28] Rezaei, M.; Warsinger, D.; Duke, M.; Matsuura, T.; Samhaber, W. Wetting Phenomena in Membrane Distillation: Mechanisms, Reversal, and Prevention. *Water Res.* 2018, *139*, 329–352. DOI: 10.1016/j.watres.2018.03.058.

[29] Tang, H.; Wang, H.; He, J. Superhydrophobic Titania Membranes of Different Adhesive Forces Fabricated by Electrospinning. *J. Phys. Chem. C.* 2009, *113*, 14220–14224. DOI: 10.1021/jp904221f.